Application of a Knowledge-Based Optimization Method for Aerodynamic Design

Michelle N. Lynde and Richard L. Campbell

NASA Langley Research Center, Hampton, Virginia, USA

Abstract

The current research is investigating the application of an optimization technique to an existing knowledge-based design tool. The optimization method, referred to as CODISC, helps improve the results from a knowledge-based design by eliminating the required advanced design knowledge, or help fine-tune a well-performing vehicle. Three CODISC designs are presented using a generic transonic transport, the Common Research Model (CRM). One design optimizes the baseline CRM to demonstrate the ability to improve a well-performing vehicle. Another design is performed from the CRM with camber and twist removed, which highlights the ability to use CODISC in the conceptual design phase. The final design implements laminar flow on the CRM, showing how CODISC can optimize the extent of laminar flow to find the best aerodynamic performance. All three CODISC designs reduced the vehicle drag compared to the baseline CRM, and highlight the new optimization technique's versatility in the aircraft design industry.

Key Words

Aerodynamic design, optimization, natural laminar flow design

Nomenclature

BLSTA3D	=	Boundary layer solver code used for stability analysis
c	=	chord length
CATNLF	=	Crossflow Attenuated Natural Laminar Flow
C_D	=	Total drag coefficient
C_{D*}	=	Total drag coefficient adjusted for total lift
CDISC	=	Knowledge-based design module
CF	=	Crossflow
C_L	=	Total lift coefficient
c_l	=	Sectional lift coefficient
c_m	=	Sectional pitching moment coefficient
CODISC	=	Knowledge-based optimization method
C_P	=	Pressure coefficient
CRM	=	Common Research Model
CRMNCT	=	Common Research Model with No Camber or Twist
LASTRAC	=	Stability analysis code used for transition prediction
NLF	=	Natural Laminar Flow
Re	=	Reynolds number based on mean aerodynamic chord
SOUP	=	Simple Optimization Utility Program, variable optimization module
SSNLF	=	CDISC flow constraint
TS	=	Tollmien-Schlichting
UDF	=	Universal Damping Function (SSNLF variable)
USM3D	=	Navier-Stokes flow solver
x/c	=	x-location nondimensionalized by local chord
X_{ca}	=	Crossflow attenuation location (SSNLF variable)

X_{shk}	=	Shock location (SSNLF variable)
X_{tr}	=	Transition location (SSNLF variable)
z/c	=	z-location nondimensionalized by local chord
η	=	Semispan location nondimensionalized by semispan length

Introduction

The aerospace industry has pursued more efficient aircraft over the last several decades amid rising fuel costs and increased environmental awareness. The aerodynamic design process of a vehicle has been an important step in maximizing aircraft efficiency, and the design method chosen can vastly impact the final product. Most designers use computational tools, such as a flow solver coupled with a design method, to perform the aerodynamic analysis and design of a vehicle.

There are a variety of computational tools for the design process available, ranging in fidelity and computational cost. Many design tools rely on numerical optimization techniques, using finite-difference methods or an adjoint solver to compute the required sensitivity derivatives. These optimization methods offer the potential to find the theoretical best performance, but can be computationally expensive and time consuming. Some optimization techniques also run the risk of producing single-point designs by introducing unconventional shapes that perform significantly worse off-design.

Another aerodynamic design tool is a knowledge-based design method that adjusts the shape of the aerodynamic surface to obtain a desired characteristic (i.e., surface pressure distribution), similar to an inverse design tool. This knowledge-based design tool, CDISC(1), can be coupled with any flow solver and uses prescribed sensitivity derivatives, thereby significantly reducing the computational cost of design by several orders of magnitude compared to traditional optimization techniques. However, unlike optimization techniques, CDISC requires the user to have some a priori knowledge of the characteristics that create an efficient vehicle. The knowledgeable user must manually adjust the CDISC input parameters to meet design goals.

The current research is investigating an optimization technique for the existing knowledge-based design tool, CDISC. Adding optimization to CDISC could help accomplish 3 goals to improve the usefulness of the design tool. First, it would eliminate the required a priori knowledge of the characteristics of a well-performing vehicle. Second, it can help fine-tune an already well-performing vehicle. Finally, it can be used to trade characteristics to maximize drag reduction, such as studying the extent of laminar flow to trade skin friction and profile drag reduction against wave drag increase. The optimization program, referred to as SOUP (Simple Optimized Utility Program), automatically adjusts the standard CDISC input variables based on the flow solver results to find the input variables that produce the lowest drag. This program eliminates the need for the user to manually adjust these input variables. The new coupled approach of using SOUP with CDISC is referred to as CODISC.

This paper will focus primarily on applications of this knowledge-based optimization method, CODISC. The applications shown will aim to evaluate the success of SOUP in accomplishing the 3 main goals to improve the usefulness of CDISC. Methods, including details on the computational tools, will be discussed, followed by the results and analysis of the 3D viscous CODISC applications. A companion paper, titled "Development of a Knowledge-Based Optimization

Method for Aerodynamic Design" by R. Campbell and M. Lynde, focuses on the technique development.

Methods

Computational tools for aerodynamic analysis and design have become increasingly available, offering a wide range of fidelity to accommodate a variety of configurations and design constraints. Effective application of such computational tools requires an understanding of the requirements and limitations of the codes. The current research is focused on developing and evaluating a new knowledge-based optimization method, CODISC. The design method and necessary supporting tools, such as the flow solver and boundary layer transition prediction software, will be discussed in this section.

A. *Computational Tools*

The computational tools required for the present research include a flow solver and a design module with a utility optimization program. The flow chart in Figure 1 illustrates the design and analysis framework. As seen in the flow chart, when performing laminar flow designs, a boundary layer stability analysis and transition prediction software package is also required. The transition prediction loop is an external process to the design loop at this time, and the loops are not performed at the same frequency. The transition prediction is performed once the design has been completed, which saves computational time and resources.

The flow solver utilized in this work is a cell-centered, finite-volume Navier-Stokes code called USM3D(2). The results presented in this paper used a tetrahedral cell grid with approximately 34.4 million cells, a y+ of 0.5 based on the distance from the surface to the first cell centroid, and approximately 30 viscous layers within the boundary layer. The Spalart-Allmaras turbulence model was used for these analyses. For laminar flow designs, the transition prediction loop is needed to model the extent of laminar flow and requires transition prediction software and the forced laminarization feature within USM3D. The transition prediction software uses two boundary layer codes, BLSTA3D(3) and LASTRAC(4). Boundary layer profiles are calculated from streamwise pressure distributions at several stations on the wing by the BLSTA3D code. The conical flow assumption, which models wing sweep and taper, is used to account for 3D effects when calculating the boundary layer profiles. These profiles are then analyzed using the LASTRAC software to determine the transition location. LASTRAC is a set of physics-based codes for stability analysis across a wide range of flow conditions and fidelity. For laminar flow designs, the e^N method is utilized, using linear stability theory with the fixed-beta method. The analysis includes compressibility effects, but no curvature effects. For transonic wings, crossflow (CF) and Tollmien-Schlichting (TS) modal instabilities are analyzed using BLSTA3D and LASTRAC. The transition location is determined as the location where the N-factor growth reaches a critical N-factor. A critical N-factor of 10 is used to represent a flight environment for both CF and TS. Once the transition location is computed at a number of stations, a transition front can be determined by linearly interpolating between the stations. The transition front is modeled within USM3D with the forced laminarization feature. This feature allows the user to input a transition front on a given surface, and the flow solver will suppress turbulence growth forward of the transition front (in the laminar region). This allows the aerodynamic effects of laminar flow to be accounted for, such as reduced skin friction and profile drag, which is necessary in order to quantify the performance benefit of sustaining laminar flow.

B. Knowledge-Based Optimization Method

The CODISC knowledge-based optimization method is built around an existing knowledge-based design tool, CDISC, with a new utility optimization program, SOUP. CDISC has been widely used over the last several decades in a variety of design applications, and has proven to be an effective and efficient design tool, often producing results comparable to traditional optimization methods. The flow constraints within CDISC allow the user to design to common aerodynamic variables, such as span load, section lift and/or pitching moment coefficients, and shock strength. CDISC geometry constraints are available to address requirements from other disciplines, such as structures and manufacturing, including thickness, curvature, volume, and leading-edge radius. CDISC automatically generates target pressure distributions from the current flow solver analysis pressures based on the user-selected flow constraints. It will then adjust the grid according to prescribed sensitivity derivatives and any user-defined geometry constraints in order to match the flow solver analysis pressures to the CDISC-generated target pressures. Typically, a design completed using CDISC is 1-3 orders of magnitude faster than numerical optimization techniques. Within each CDISC flow and geometry constraint, there are several variables that the user can adjust that alter the target pressures. To begin a design, a CDISC user will select several flow and geometry constraints, and associated constraint variables, that will produce target pressure distributions to support the design goals. An automated setup process is being developed that will generate a standard set of flow and geometry constraints for a new user. Tweaking the constraint variables is typically done manually by the user based on previous experience with aerodynamic design. When using the new CODISC optimization method, SOUP will adjust the constraint variables automatically to minimize total vehicle drag.

Each CDISC constraint has a variety of variables that can be adjusted to change the design. SOUP works by optimizing one of these variables within a designated CDISC flow constraint (thereby adjusting the target pressure distribution) to reduce drag. SOUP is a simple auxiliary code that compares the drag between the current and previous design cycles, then alters the selected variable accordingly with the goal of reducing the drag. The drag that SOUP evaluates can either be the total configuration drag or the local drag calculated from integrated pressure and skin-friction at designated spanwise stations. In order to ensure a change in drag is related to a change in the variable, SOUP does not alter a variable until the analysis pressures closely match the target pressures (quantified by the computed total lift closely matching the specified design total lift). SOUP adjusts the drag value used within the optimization algorithm to account for changes in drag due to mismatching design lift. This technique has proven to make the optimization process more robust, as it minimizes the susceptibility to changing the variable in the incorrect direction due to mismatching lift (and therefore drag) values. In addition to driving the direction of the variable change, the adjusted drag value determines when the CODISC optimization process is complete. CODISC will continue adjusting the variable (subject to variable maximum/minimum limits when necessary) until a minimum drag or a flat minimum drag has been detected. The minimum drag criteria will terminate the CODISC process when the variable changes have caused an increase in drag (by a user-specified amount) compared to the previous minimum drag. The flat minimum drag criteria will trigger the end of the CODISC process when the drag remains unchanged (within a user-specified variation) for at least 10 optimization cycles. The user-specified drag limits for both minimum detectors should be large enough to avoid early termination of the CODISC process due to noise in the drag values.

One CDISC flow constraint, called SSNLF, has been widely used for both laminar and turbulent designs on transonic and supersonic vehicles(5-8). The SSNLF constraint has several variables associated with it; how the variables are used differ based on the type of design (laminar or turbulent). A sample target pressure distribution using SSNLF for turbulent flow can be seen in Figure 2, and a laminar flow sample target pressure distribution is shown in Figure 3. The laminar flow technology used in the SSNLF constraint is referred to as Crossflow Attenuated Natural Laminar Flow (CATNLF), and was previously used to design a natural laminar flow wind tunnel model(7). The CATNLF method relies on pressure architecture and geometry constraints to control several mechanisms of transition, including attachment line transition, Görtler vortices, and modal instabilities. In Figures 2 and 3, the SSNLF constraint variables are labeled. The variable nearest the leading edge, X_{ca}, is used in laminar designs for CF attenuation by creating rapid acceleration very near the leading edge (seen in Figure 3). For turbulent designs, the X_{ca} variable can be further aft, resembling more traditional accelerations for transonic airfoils. The variable related to transition location, X_{tr}, is used for laminar designs to designate the end of desired laminar flow. Between X_{ca} and X_{tr} is a variable called the Universal Damping Function (UDF), which determines the pressure gradient in this region. For turbulent designs, the UDF is used to reduce shock strength, whereas in laminar designs, the UDF is used to delay transition due to TS growth. The last variable, X_{shk}, designates the shock position, and is determined within CDISC based on a function of Mach number. The X_{shk} can be updated during the CODISC process if necessary to accommodate differences between the current analysis shock location and the CDISC prescribed location. This feature increases the stability of the CODISC process. For laminar designs, there is a mild adverse pressure gradient between X_{tr} and X_{shk} to ensure boundary layer transition prior to the shock and to reduce the shock strength. That region is unnecessary in turbulent designs, so the X_{tr} and X_{shk} are set equal. As mentioned previously, a variable is optimized using SOUP to automatically alter the target pressure distributions to reduce drag. The type of design, such as laminar or turbulent, will determine which variable is optimized.

When performing a turbulent wing design, the UDF variable is selected for optimization because of its strong influence on the wave drag of the vehicle. The remaining SSNLF variables are determined internally based on empirical data from previous CDISC designs. For example, X_{ca} is a function of the maximum thickness, the X_{shk} is a function of Mach number, and the aft loading is based on the ratio of sectional lift coefficient to pitching moment coefficient. The effect of changing the UDF variable on a target pressure distribution is illustrated in Figure 4. This figure shows the direct impact on shock strength from altering the UDF variable. Two examples of turbulent design that optimize the UDF variable will be shown in the following section.

For laminar wing designs, the X_{tr} variable is selected for optimization to find the ideal extent of laminar flow. Sustaining laminar flow can increase wave drag due to the favorable pressure gradients often needed to control TS growth. There is a tradeoff between the drag-saving benefits of extended laminar flow, and the increased wave drag that often accompanies it. Optimizing the X_{tr} variable will find the extent of laminar flow that produces the minimum total vehicle drag. As mentioned, the region between X_{tr} and X_{shk} has an adverse pressure gradient to avoid laminar flow separation at the shock and to reduce the shock strength. For laminar designs, CDISC automatically calculates a UDF value that provides the necessary pressure gradient that causes TS transition at a designated X_{tr} (i.e., TS N-factor growth reaches the critical N-factor at the X_{tr}

location) and is a function of Reynolds number, critical N-factor, and X_{tr}. Figure 5 illustrates how changing X_{tr} alters the target pressure distribution, highlighting how the X_{tr} location affects the shock strength. The CDISC process will automatically update the transition front for USM3D to be the X_{tr} locations so the proper extent of laminar flow is modeled for each design optimization cycle. Upon completion of the design, the user verifies the transition location using the LASTRAC stability analysis process. The effectiveness of the laminar CODISC designs relies on how accurately the UDF can produce pressure distributions that cause transition at designated locations. Figure 6 shows a comparison of the analyzed transition location (LASTRAC analysis of the target pressure distribution) versus the desired transition location (X_{tr} value used in UDF to produce the target pressure distribution). This figure illustrates how accurately the UDF can produce pressure distributions that transition due to TS growth at designated locations at a variety of Reynolds numbers. One example of laminar design while optimizing the X_{tr} variable will be shown in the following section.

The applications of CODISC presented in this paper utilize the methods described in this section. Additional detail on the methods and development of CODISC can be found in the companion paper, titled "Development of a Knowledge-Based Optimization Method for Aerodynamic Design" by R. Campbell and M. Lynde.

Results
The CODISC knowledge-based optimization method was developed to increase the effectiveness of the CDISC design tool. The first goal of the optimization method was to eliminate the need for a priori knowledge in using a knowledge-based design tool. The second was to find improvements to a well-designed configuration that may not be immediately apparent to a designer. The final objective was to use CODISC to optimize specific aerodynamic characteristics, such as laminar flow extent where it is necessary to trade reduced skin friction and profile drag against increased wave drag. To evaluate the effectiveness of CODISC in accomplishing these goals, three optimizations were performed.

All three examples use the Common Research Model (CRM)(9) as the baseline configuration. The CRM is a generic transonic transport that has been the focus of several studies, including previous optimization work. The design conditions are Mach 0.85, lift coefficient of 0.50, and Reynolds number of 30 million based on reference chord length. Figure 7 shows a planform view of the CRM with the twelve design stations used during the CODISC optimizations. Results will be shown from two spanwise design stations, highlighted in the figure, and labeled Station 3 (inboard) and Station 9 (outboard).

A.   Turbulent Optimization Examples
The CDISC design method has had significant success in designing efficient configurations over the last several decades. As CDISC is a knowledge-based method, user expertise is required to be most effective. The CODISC optimizer extends the potential of CDISC to users who lack prior experience with aerodynamic design. To evaluate the usefulness of CODISC in eliminating the required a priori knowledge, a turbulent transonic wing design is performed on a representative conceptual stage vehicle.

An optimization method was used to develop the baseline CRM wing; to better represent a conceptual stage vehicle, the wing camber and twist have been removed for this example. The standard set of CDISC geometry constraints for turbulent design was selected to ensure realistic airfoil geometries, including curvature limits and geometry smoothing. The maximum thickness and leading-edge radius were held constant at each station (chordwise location of maximum thickness was free to move), and the sectional lift coefficients were set to maintain the baseline CRM spanwise loading distribution. For the flow constraint, the SSNLF constraint is used as previously described in the Methods section for turbulent design. The UDF variable is selected as the SOUP optimization variable, with the total vehicle drag (adjusted for lift changes) used as the driver. For the spanwise UDF distribution, previous investigations have suggested a linear distribution, anchored at UDF = 0 at the wing tip, with a maximum UDF value of 1 at any station, produces consistently good results. This linear distribution was found to be more stable and better performing than when the UDF was free to change locally at each station. Additional detail on the development of this UDF distribution can be found in the companion paper, titled "Development of a Knowledge-Based Optimization Method for Aerodynamic Design" by R. Campbell and M. Lynde. For this example, the initial UDF values are set low, and SOUP will continue to increase the values until a drag minimum is detected.

The baseline solution of the CRM with no camber/twist (CRMNCT) was obtained, and then the CODISC optimization run was submitted for 100 optimization cycles. The configuration was held at an angle of attack of 1.96 degrees throughout the run, which is the angle of attack needed for the baseline CRM to obtain the design lift coefficient of 0.50. The CODISC stop criteria was reached after 62 optimization cycles when a minimum value was detected for the total drag. Figure 8 shows the changes in pressure distribution and airfoil geometry at two spanwise stations between the initial CRMNCT geometry (Baseline) and the CODISC optimized geometry (Design). The airfoil geometries (right) are plotted with the twist removed and x- and y-axes scaled differently to better show the shape changes between the airfoils. This comparison shows how CODISC added camber back into the geometry to produce airfoils that resemble typical transonic supercritical airfoils. The CODISC process drove the inboard stations of the Design to be shock-free and outboard stations to have weak shocks to reduce wave drag. Further comparisons of the initial CRMNCT (Baseline) and CODISC optimized (Design) geometries are shown in several spanwise distributions in Figure 9.

For a turbulent design, the UDF variable is selected as the optimization variable and increased according to total drag. The variable and force history (lift on left, drag on right) during the optimization process can be seen in Figure 10. The optimized variable did not begin to change until the total lift was acceptably close to the design lift (shown as C_L convergence bands on the left plot) at cycle 14. This criteria ensures the current analysis pressures are close enough to the target pressures so the changes in drag are due to the change in the UDF variable. The figure also shows the total drag (C_D) and adjusted drag (C_{D*}) history. The drag continues to decrease as the UDF variable increases, until a minimum is reached at cycle 55. The CODISC stop criteria for this case was set to end the optimization process when the total adjusted drag, C_{D*}, increased by a half count of drag ($C_D = 0.00005$), which is reached at cycle 62. The UDF values in Figure 10 are the UDF values at the root for each design cycle. The root station determines the UDF values at other stations because a linear distribution of UDF values is used from the root value to 0 at the tip. As seen in the figure, the root UDF value reaches the maximum allowed value (UDF = 1) at cycle 50.

Once the root station reaches the maximum UDF value, the stations outboard can continue to increase, maintaining the linear distribution with the next station outboard. This can continue until all stations are limited by the maximum UDF value of 1 (or until the optimization stop criteria occurs). Figure 11 shows the initial and optimized spanwise distribution of the UDF variable. It can be seen that the inboard two stations of the optimized distribution reached the maximum UDF value, with the linear distribution between station 3 and the tip.

The CODISC optimization of the CRMNCT successfully decreased the drag coefficient to 0.02321 at the design lift ($C_L = 0.50$) as shown in Figure 10. For comparison, the baseline CRM, which is a well-performing transonic transport, has a drag coefficient of 0.02357 at the design lift. The CODISC process was able to take a representative conceptual stage vehicle and improve the drag by 3.6 counts (1.5%) compared to the baseline CRM. The optimization was completed in 31,000 flow solver iterations, which is approximately 1-2 times a standard analysis time for a configuration. The improvement was obtained without user intervention, which supports the goal of extending CDISC to inexperienced designers for use in the conceptual design stage.

Another motivation for developing the CODISC knowledge-based optimization method was to find improvements to a well-designed configuration that may not be immediately apparent to a designer. To evaluate this goal, a second turbulent design was performed. The baseline for this optimization was the unaltered CRM configuration. This vehicle was previously designed using an optimization method, and represents a well-designed configuration. This example also helps evaluate if the starting point influences the final optimized design, as the optimization is set up identically in the two examples, with only the baseline configuration changing.

The same standard set of CDISC flow and geometry constraints were utilized in this optimization as the previous example. This includes curvature limits and geometry smoothing, as well as holding maximum thickness, leading-edge radius, and sectional lift coefficients constant. For this turbulent design example, the UDF variable was again set as the optimized variable and the adjusted total drag was used for both the variable optimization and the CODISC stop criteria. The baseline CRM solution was obtained and the CODISC optimization was submitted, holding angle of attack constant throughout the process. After 66 optimization cycles, the stop criteria was reached. The optimized pressure distributions and airfoil shapes at two spanwise stations are shown in Figure 12. While the differences between the baseline CRM (Baseline) and the CODISC optimized (Design) configurations are less severe, similar features can be seen in this example in the design results, such as shock-free pressures and increased aft loading inboard. The spanwise characteristics in Figure 13 show minimal changes between the baseline and design configurations.

The CODISC process increased the UDF values until a minimum drag was detected. The UDF and force history (lift in the left plot, drag in the right plot) for this example are shown in Figure 14. Since this optimization was started from a much better vehicle, the time to get within the lift requirement (shown as C_L convergence bands on the left plot) was much shorter than the previous example. In 5 optimization cycles, SOUP began to increase the UDF values. By cycle 42, the root station UDF value had reached the maximum value of 1. The UDF values at the outboard stations continue to increase until the stop criteria is reached at cycle 66, when the adjusted drag, C_{D*}, had increased by half a count ($C_D = 0.00005$) from the previous minimum, seen at cycle 53. The final spanwise distribution of UDF values is shown in Figure 15. In this example, the inboard 3 stations

reached the maximum UDF value, with the linear distribution between station 4 and the tip. The difference between the UDF distributions for the two turbulent design examples suggest the initial configuration can impact the optimization results.

The CODISC optimization from the baseline CRM had a drag coefficient of 0.02330 at the design lift coefficient of 0.50 as shown in Figure 14. While this is slightly less than the improvement seen when starting from the CRMNCT configuration, the optimization still improved the CRM by 2.7 drag counts (1.2%). The optimization process took 33,000 flow solver iterations (approximately 1-2 times a standard flow analysis time). The results from this CODISC example support the goal of using the optimization tool to find improvements to well-performing vehicles. A summary of the performance improvement of the two turbulent examples can be found in Table 1.

One potential risk of using an optimizer for aerodynamic design is producing single point designs, configurations that perform significantly worse at off-design conditions. The optimized pressure distributions for both examples had shock-free airfoils inboard, and a common concern with this type of pressure distribution is the off-design performance. To investigate the off-design performance of the two CODISC results, near-cruise conditions were analyzed, seen in the drag polar plot in Figure 16. The configurations were analyzed at a wide range of C_L values, but the near-cruise condition of ±10% design C_L is of most interest. The drag polar plot shows both optimized configurations performed very similarly across all C_L values analyzed. At higher C_L values, the optimized configurations performed better than the baseline CRM. However, at lower C_L values, the optimized configurations performed slightly worse than the baseline CRM. A summary of the near-cruise lift and drag values can be found in Table 2. The configurations were also analyzed at different Mach numbers at the design lift coefficient, the results of which are shown in the drag rise plot in Figure 17. This plot shows the optimization method increased the Mach number at which drag rise occurs. There is a notable difference in drag between the two optimized configurations at the lower Mach numbers, which is being further investigated. In general, the initial investigation of off-design performance of the two optimized configurations appear positive, showing sustained aerodynamic improvement compared to the baseline CRM at most conditions. This suggests the CODISC method produces robust designs similar to the traditional CDISC method.

The two turbulent optimization examples from this section support the first two goals of the CODISC knowledge-based optimization method. To evaluate if CODISC can replace the a priori knowledge required for a knowledge-based design method, the optimization tool was used to design a conceptual design stage vehicle (in this case, the CRM with no camber or twist). To evaluate if CODISC can improve upon a well-performing vehicle, the optimization tool was used to design the CRM. Both examples optimized the UDF variable in the SSNLF constraint to find drag reduction when compared to the baseline CRM configuration. The performance improvement was sustained at most near-cruise conditions in both lift and Mach variations. The two optimized configurations had slightly different performance, suggesting the starting configuration can impact the final design. However, both configurations achieved the goal of performance improvement compared to the baseline CRM, and this suggests CODISC is an effective tool to use in both the conceptual and preliminary stages of vehicle design.

B. Laminar Optimization Example

Often in the aerodynamic design process, the designer must trade specific features to find the optimum performance benefit. This task can often be time consuming, requiring comparing several designs to find the best. One potential benefit of the CODISC knowledge-based optimization method is the ability to use the tool to quickly find the optimum performance benefit that a feature can provide. One such example is optimizing the extent of laminar flow. Sustaining laminar flow provides significant drag savings through decreased skin friction and profile drag. However, laminar flow can often lead to increased wave drag due to the favorable pressure gradients required to control TS growth. The goal is to use CODISC to determine the optimum extent of laminar flow on total drag.

To evaluate the ability to find the optimum extent of laminar flow, a laminar design is conducted using CODISC. Similar to the previous turbulent examples, the baseline configuration is the CRM, and the SSNLF flow constraint is used. However, this example will use the laminar flow design option within the SSNLF constraint. The X_{ca} will be forward for CF attenuation, and the UDF will be internally determined by CDISC to delay TS transition to the desired transition location, X_{tr}. There will be a region of at least 10% chord of adverse pressure gradient between X_{tr} and X_{shk} to reduce the shock strength. Since the shock location is determined internally based on a function of Mach number, the extent of laminar flow can be aft limited by the shock due to the minimum required 10% chord of adverse pressure gradient. For this example, the transition location, X_{tr}, is selected as the optimization variable for CODISC. Unlike the turbulent examples, the X_{tr} optimization is based on sectional drag, which is calculated at each station by integrating skin friction and pressures. CODISC will continue to increase the extent of laminar flow at each station based on the local drag at the station until the local drag increases or the X_{tr} is within 10% chord of the X_{shk}. The CODISC stop criteria is based on total adjusted drag when a minimum is detected.

For laminar design, a few additional CDISC geometry constraints are needed. In addition to the standard curvature constraints used in turbulent design to keep the airfoils reasonable, another curvature constraint to eliminate concavity in regions of laminar flow is required to address transition due to Görtler vortices. Additionally, attachment line transition is addressed with a leading-edge radius constraint that reduces the radius to avoid attachment line transition. For this example, it is assumed that an external device could be used to address attachment line contamination due to a turbulent fuselage boundary layer. Therefore, the leading-edge radius constraint is only needed to avoid attachment line transition. The flow solver uses a transition front associated with the current cycle X_{tr} values. The CODISC process was started for 100 optimization cycles with a constant angle of attack from the baseline turbulent CRM solution. The pressure distributions and airfoil shapes can be seen in Figure 18. The Design has faster acceleration near the leading edge and stronger shocks compared to the Baseline, which is expected for a laminar configuration. The spanwise characteristics of the two configurations are compared in Figure 19. As mentioned, the leading-edge radius of the Design is reduced to avoid attachment line transition, as well as to help obtain the rapid acceleration needed for CF attenuation.

For laminar design, the optimized variable was adjusted individually at each station based on local drag. Figure 20 shows an example of how the X_{tr} variable changed at one station (root station shown), along with the total vehicle lift and drag history (lift on left, drag on right). The optimized variable, X_{tr}, was held constant at every station until the total lift was within the accepted range.

The acceptable C_L convergence range for this example was much smaller due to the fact the laminar designs require closer matches to target pressures because laminar flow is very sensitive to pressure gradients. The smaller C_L convergence range increased the time the variables were held constant to cycle 28. The stop criteria was reached after 75 optimization cycles, with an increase in adjusted drag (C_{D*}) of half a count ($C_D = 0.00005$) from the minimum that occurred at cycle 64. The computational time required to perform 75 optimization cycles represents approximately 2 times that of a standard analysis. The optimized spanwise distribution of X_{tr} can be seen in Figure 21. The stations outboard of 73% span had the transition location limited by the shock location, as discussed previously. The final design sustained laminar flow on 45% of the surface area of the wing upper surface. The drag coefficient for the optimized configuration was 0.02244 at the design lift, as seen in Figure 20, which represents a performance improvement of 11.3 drag counts (4.8%) from the baseline CRM.

A key factor in the ability to optimize transition location is that the configuration would actually transition at the desired X_{tr} (meaning the relationship between laminar flow penalties and benefits are modeled correctly). To evaluate this, the final Design configuration was analyzed using the stability analysis and transition software described previously. Figure 22 shows three transition fronts, one created from the final optimized transition locations (X_{tr}) and the other two from LASTRAC predicted transition locations of the final flow solver pressures (Design) and the final target pressures (Target). Attachment line, Görtler vortices, CF, and TS transition mechanisms were evaluated to create these transition fronts. Comparing the transition fronts from the target pressures (green line) and the X_{tr} values (blue line) shows how accurate the internally calculated UDF values are. Across the span, the analyzed target pressure transition location and the X_{tr} values are within an average of 5% chord. This accuracy suggests the internal UDF calculator produces adequate target pressures for desired extents of laminar flow at a wide range of Reynolds numbers across the span of the wing. The analyzed transition locations from the final design flow solver pressures closely match both the X_{tr} values and the target pressure transition locations across the span, except inboard at Station 2. The closeness of the Design (red line) and X_{tr} values (blue line) across the span suggests that the modeled transition front in the flow solver (which directly impacts the aerodynamic performance that is driving the optimizer) is an adequate representation for optimization. Omitting the discrepancy at Station 2, the Design (red line) and Target (green line) transition locations across the span were within an average of 3% chord. This suggests that, in general, the analysis pressures closely matched the target pressures. A closer look at Station 2 was needed to determine the reason for the large mismatch in transition location. Figure 23 compares the Design and Target pressure distributions (left plot) and the TS N-factor growth (right plot) at Station 2. The image shows the Design pressures have a less favorable pressure gradient than the Target pressures between the leading edge and approximately 25% chord. This decreased favorable pressure gradient causes the TS to grow more rapidly on the Design, leading to premature transition (seen in the right plot). This discrepancy in pressure gradient was isolated to the inboard Station 2. In general, the stability analysis and transition prediction results from this example show that the transition locations were adequately modeled during the optimization process. This suggests that the CODISC process captures the relationship between the benefits and penalties of sustaining laminar flow well enough to optimize the extent of laminar flow.

The CODISC knowledge-based optimization method was applied to a laminar design in order to find the optimum extent of laminar flow. The SSNLF constraint was used for laminar design, and

the Xtr variable was optimized at each spanwise station. The results demonstrated significant extents of laminar flow that lead to drag savings compared to the baseline CRM configuration. Further analysis of the final design suggests the design matched the target pressures well and the appropriate extents of laminar flow were modeled in the flow solver. The results thus far demonstrate the ability to use CODISC to optimize the extent of laminar flow.

Concluding Remarks

The need for better performing aircraft has led to the advancement of several aerodynamic design capabilities. One such capability is numerical optimization, which can design efficient vehicles, but often with increased computational cost. The CDISC knowledge-based design method has been a viable option to maximize performance while maintaining reasonable computational cost over the past several decades. However, a knowledge-based tool inherently requires the user to have a priori knowledge of vehicle design. A new knowledge-based optimization method, CODISC, has been created with the goal of improving the current CDISC capabilities. This paper focused on applications of this new optimization method, showing several 3D examples to evaluate the new tool.

Two turbulent designs were performed to evaluate the first two goals of the CODISC knowledge-based optimization method. The first goal of CODISC is to extend the design capabilities of CDISC to inexperienced users. To evaluate this goal, an optimization was performed on a representative conceptual design stage vehicle. The Common Research Model (CRM) was used as the baseline configuration, but to better represent a conceptual design stage vehicle, the wing camber and twist were removed. The second goal of CODISC is to find additional performance improvements to an already well-designed vehicle, so the second example was a CODISC optimization of the unaltered CRM. In both examples, CODISC was used to optimize a variable that significantly impacts the wave drag. Both optimization cases produced similar turbulent designs, showing similar pressure distributions and airfoil characteristics. The two designs had improved performance compared to the baseline CRM. An initial investigation on the off-design performance of the optimization results suggest sustained drag reduction at most conditions.

A third CODISC application was presented using the laminar flow design capability within CDISC. This example aimed to evaluate the goal that CODISC can be used to perform trades for specific characteristics. In this case, the extent of laminar flow was optimized, trading the benefits of laminar flow on skin friction and profile drag against the penalties on wave drag. The laminar design had significant drag savings compared to the baseline CRM. The results suggest the successful application of CODISC to optimize the extent of laminar flow. In addition, the analyses demonstrated the accuracy of the laminar flow design capability with CDISC.

Several applications of the new knowledge-based optimization method, CODISC, were shown to evaluate the viability of using the method in a design environment. Preliminary results suggest the method has significant promise to improve the usefulness of the CDISC design module and highlight the versatility of the method in the aircraft design industry. Additional applications of CODISC and any possible improvements discovered will help further develop this promising optimization method.

References

1. Campbell, R. L., "Efficient Viscous Design of Realistic Aircraft Configurations," AIAA-98-2539, June 1998.
2. Frink, N. T., Pirzadeh, S. Z., Parikh, P. C., Pandya, M. J., and Bhat, M. K., "The NASA Tetrahedral Unstructured Software System," The Aeronautical Journal, Vol. 104, No. 1040, October 2000, pp.491-499.
3. Wie, Y.-S., "BLSTA: A Boundary Layer Code for Stability Analysis," NASA CR 4481, 1992.
4. Chang, C.-L., "The Langley Stability and Transition Analysis Code (LASTRAC): LST, Linear and Nonlinear PSE for 2-D, Axisymmetric, and Infinite Swept Wing Boundary Layers," AIAA 2003-0974, 2003.
5. Lynde, M.N. and Campbell, R.L., "Expanding the Natural Laminar Flow Boundary for Supersonic Transports", 34th AIAA Applied Aerodynamic Conference, AIAA AVIATION Forum, AIAA 2016-4327, June 2016.
6. Campbell, R.L., and Lynde, M.N., "Natural Laminar Flow Design for Wings with Moderate Sweep", 34th AIAA Applied Aerodynamic Conference, AIAA AVIATION Forum, AIAA 2016-4326, June 2016.
7. Lynde, M. N., and Campbell, R. L., "Computational Design and Analysis of a Transonic Natural Laminar Flow Wing for a Wind Tunnel Model," AIAA-2017-3058, June 2017.
8. Campbell, R. L. and Lynde, M. N., "Building a Practical Natural Laminar Flow Design Capability," AIAA-2017-3059, June 2017.
9. Vassberg, J. C. and Rivers, S. M., "Development of a Common Research Model for Applied CFD Validation", AIAA 2008-6919, August 2008.
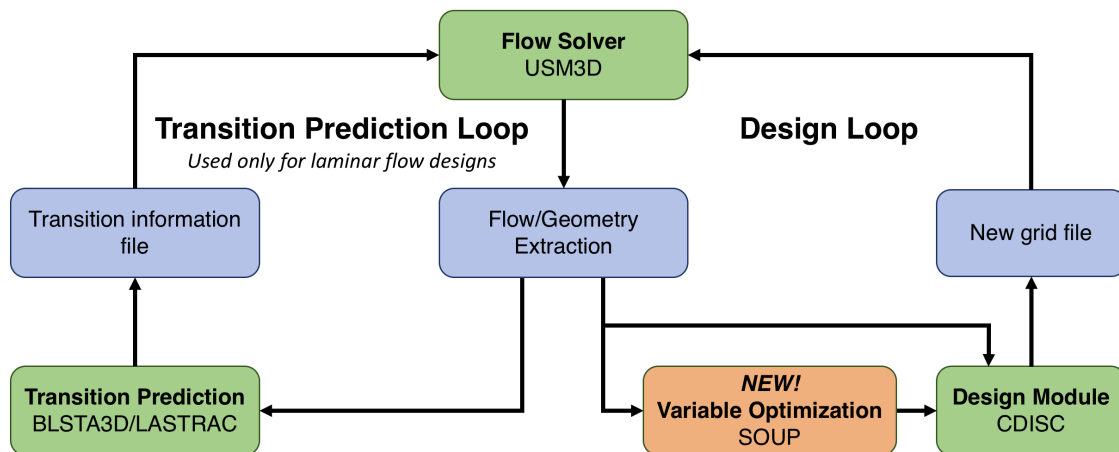
Figure 1. Flow chart of CODISC knowledge-based design method.
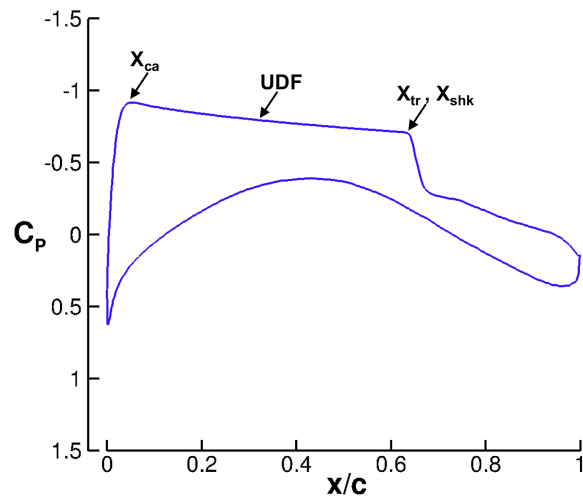
Figure 2. A sample transonic target pressure distribution showing the CDISC variables used in the SSNLF flow constraint for turbulent flow design.
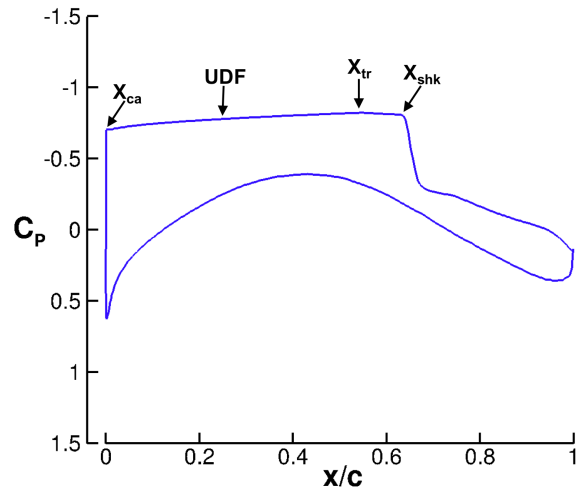
Figure 3. A sample transonic target pressure distribution showing the CDISC variables used in the SSNLF flow constraint for laminar flow design.
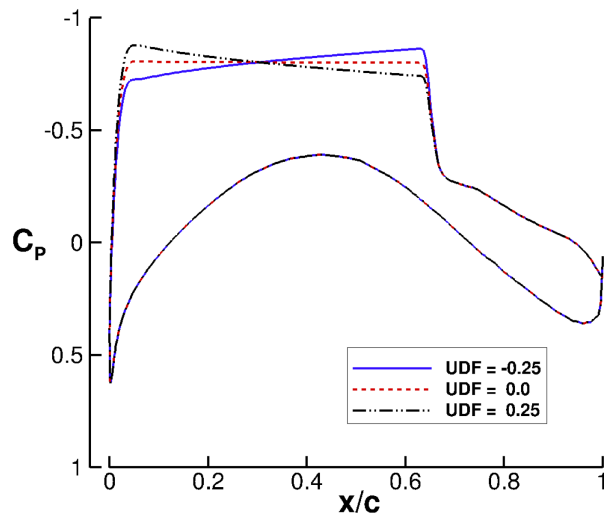
Figure 4. A sample turbulent target pressure distribution showing the effect of changing the UDF variable within the SSNLF flow constraint.
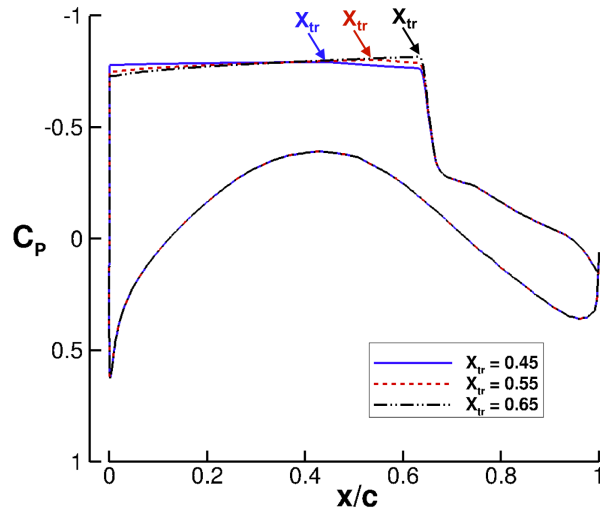
Figure 5. A sample laminar target pressure distribution showing the effect of changing the X_{tr} variable within the SSNLF flow constraint.
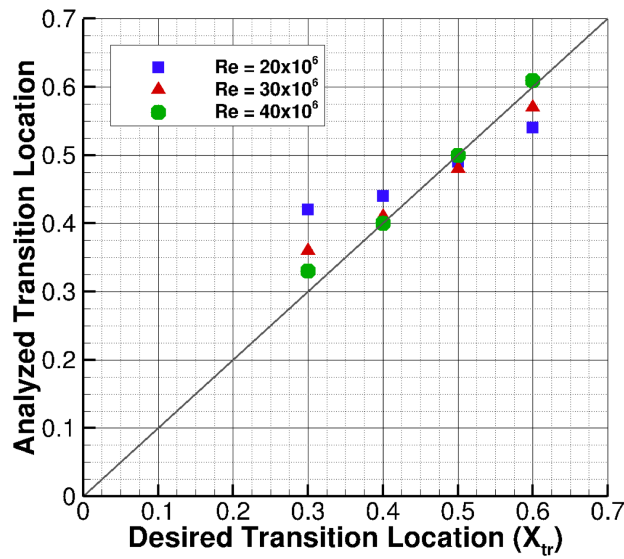
Figure 6. Comparison of the analyzed transition location (computed using LASTRAC on the target pressure distribution) and the desired transition location (X_{tr} values used to create target pressure distribution) at a variety of relevant Reynolds numbers.
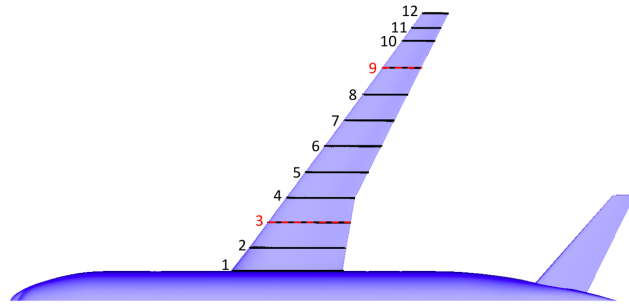
Figure 7. Planform view showing the design stations on the CRM configuration. Results will be shown for Station 3 and Station 9 (highlighted in red).
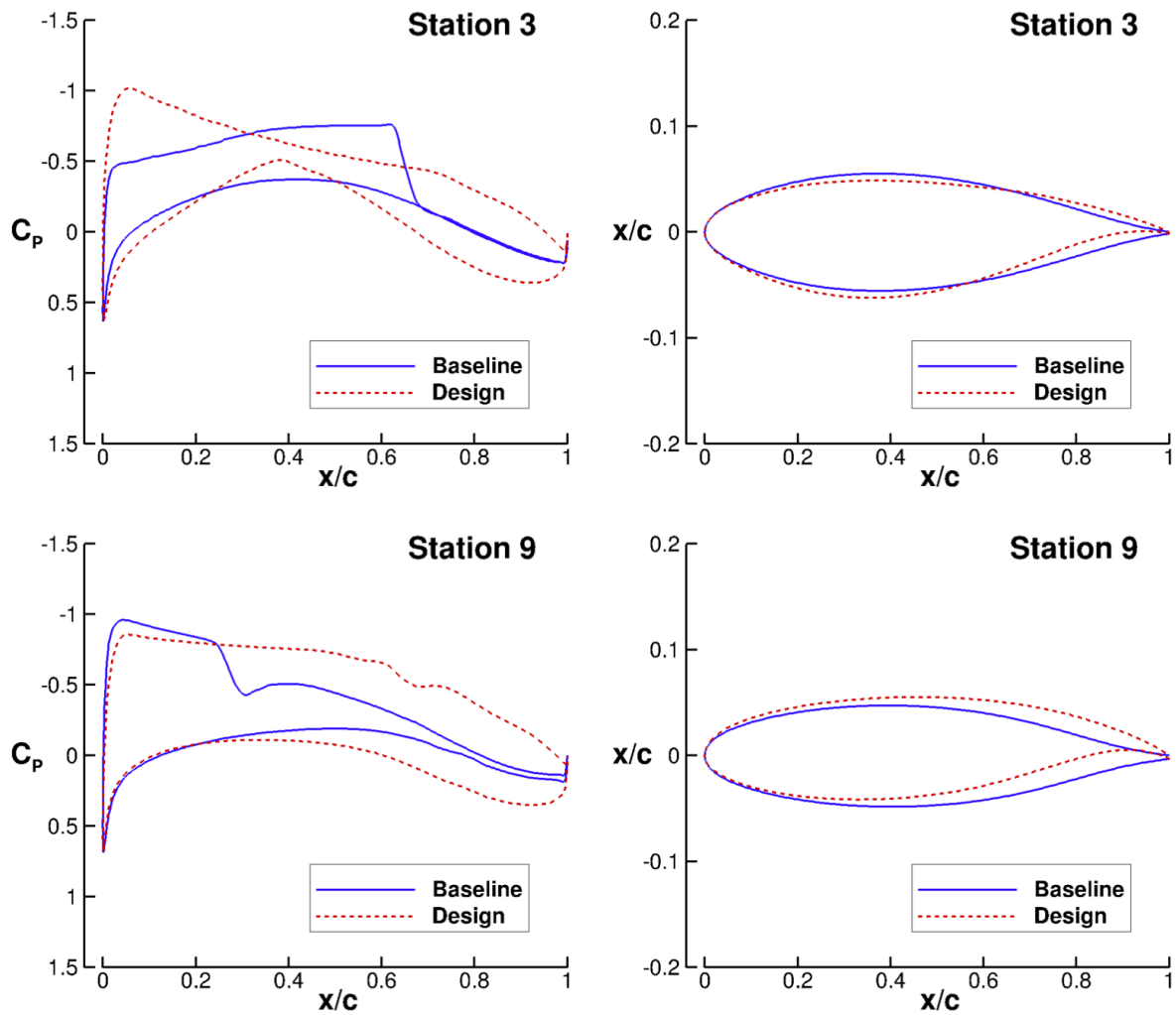
Figure 8. Comparison of the pressure distribution (left) and airfoil shape (right) of the initial CRMNCT (Baseline) and CODISC optimized (Design) configurations at Station 3 (top) and Station 9 (bottom).
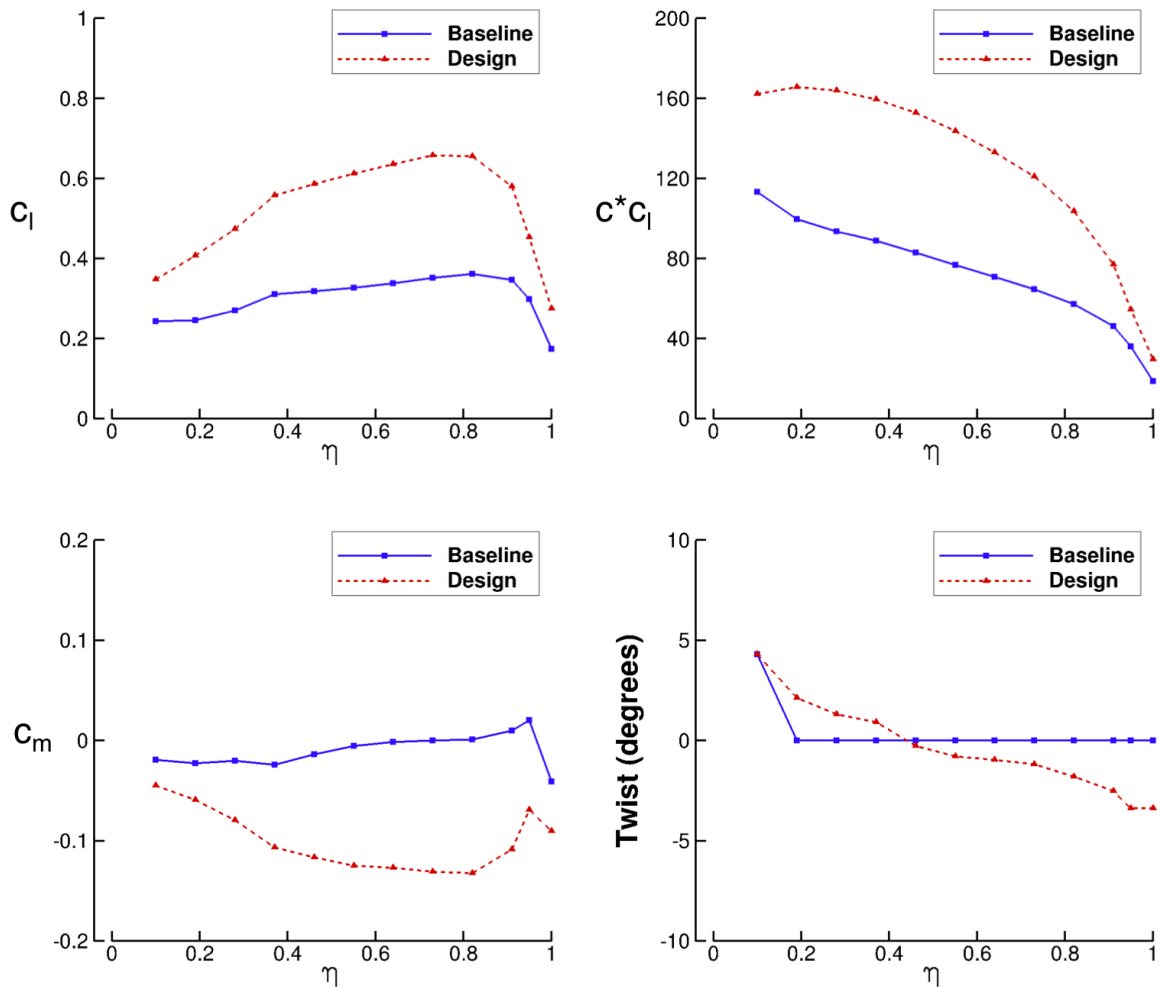
Figure 9. Comparison of spanwise characteristics of the initial CRMNCT (Baseline) and CODISC optimized (Design) configurations at Station 3 (top) and Station 9 (bottom).
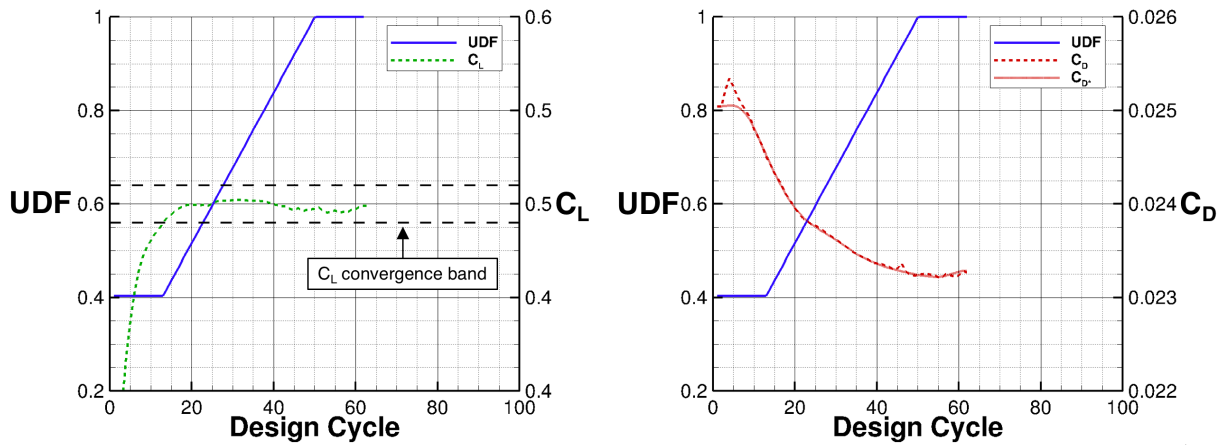
Figure 10. History of the optimized variable (UDF) and the total forces (lift on left, drag on right) during the CODISC optimization process.
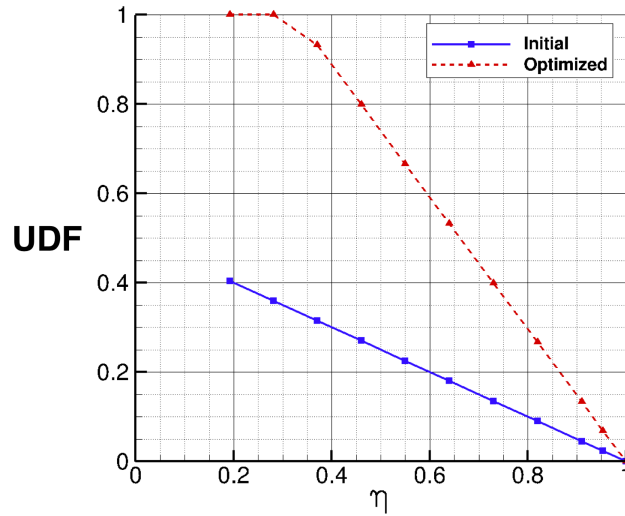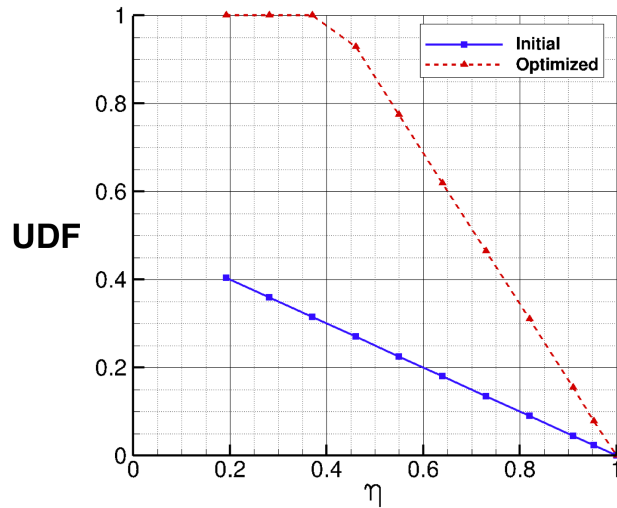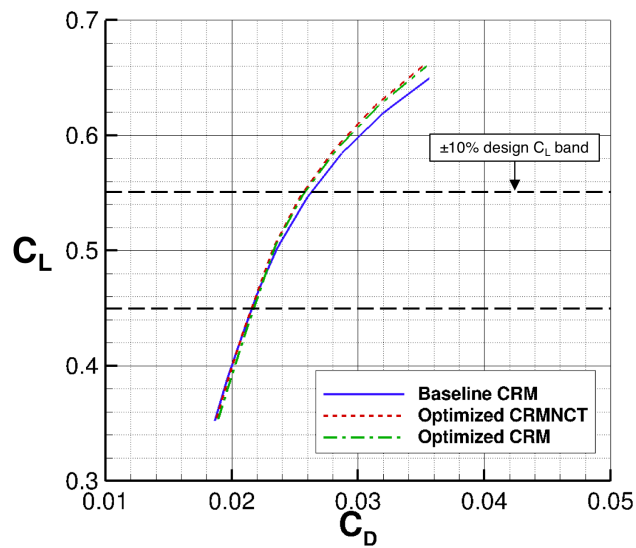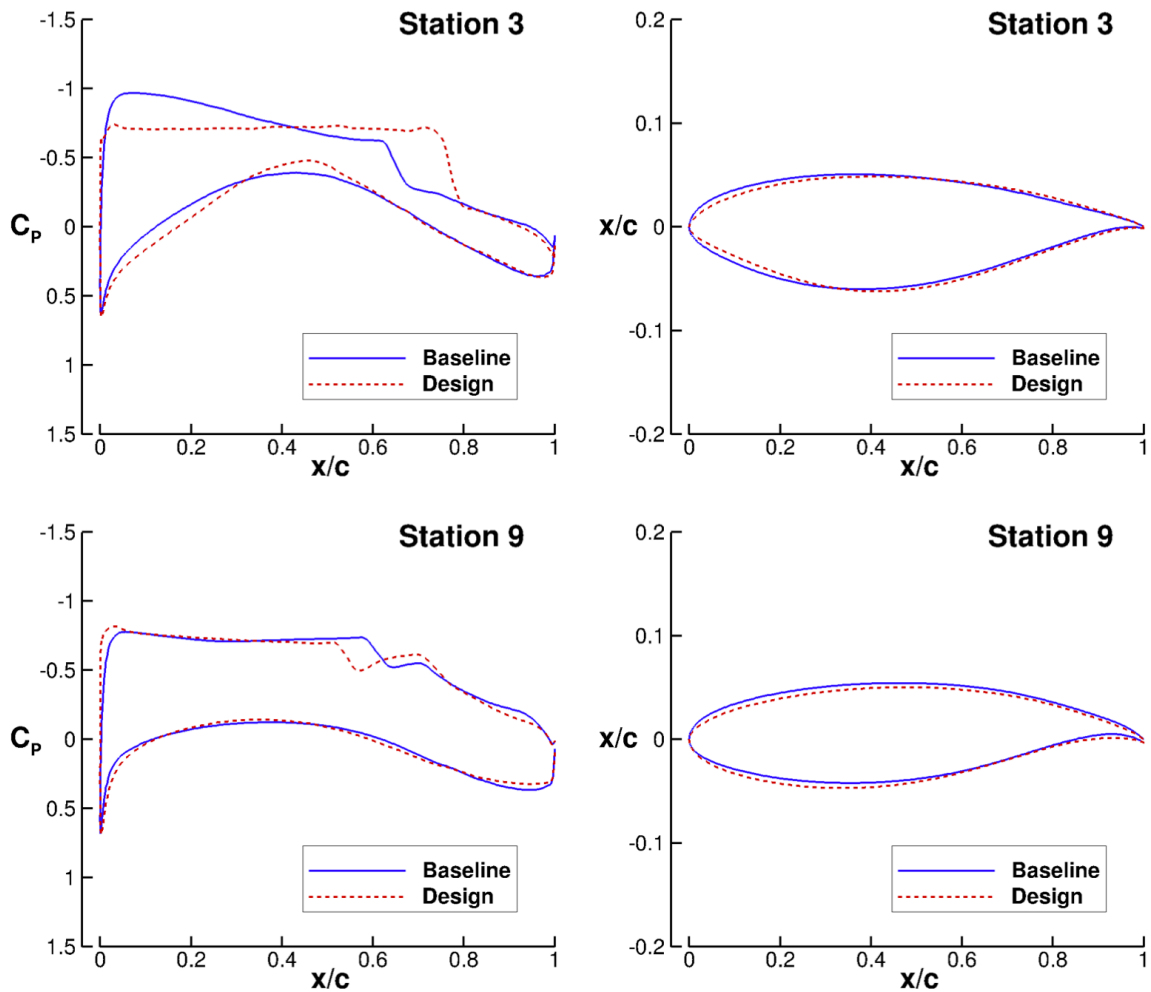
Figure 11. Spanwise distribution of the UDF variable.
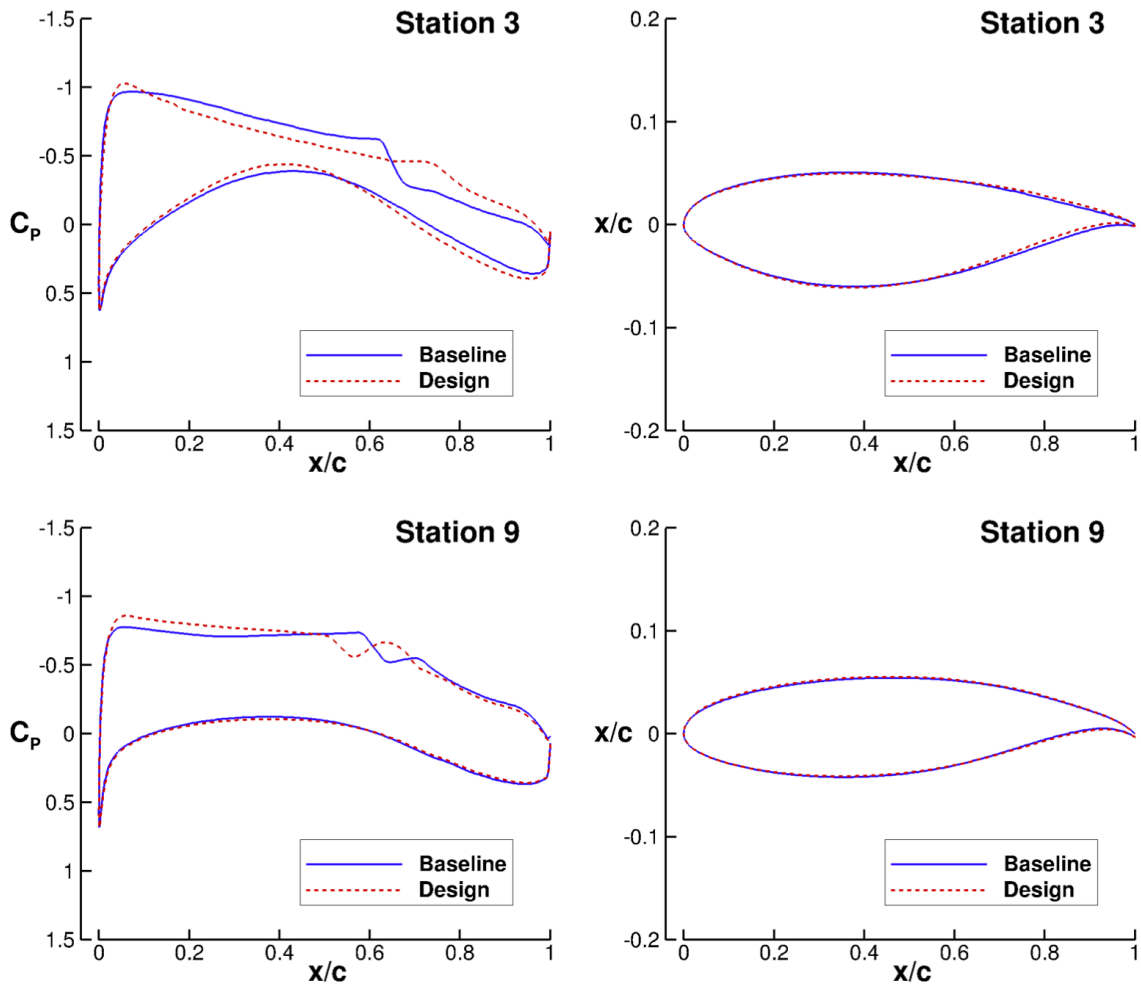
Figure 12. Comparison of the pressure distribution (left) and airfoil shape (right) of the initial CRM (Baseline) and CODISC optimized (Design) configurations at Station 3 (top) and Station 9 (bottom).
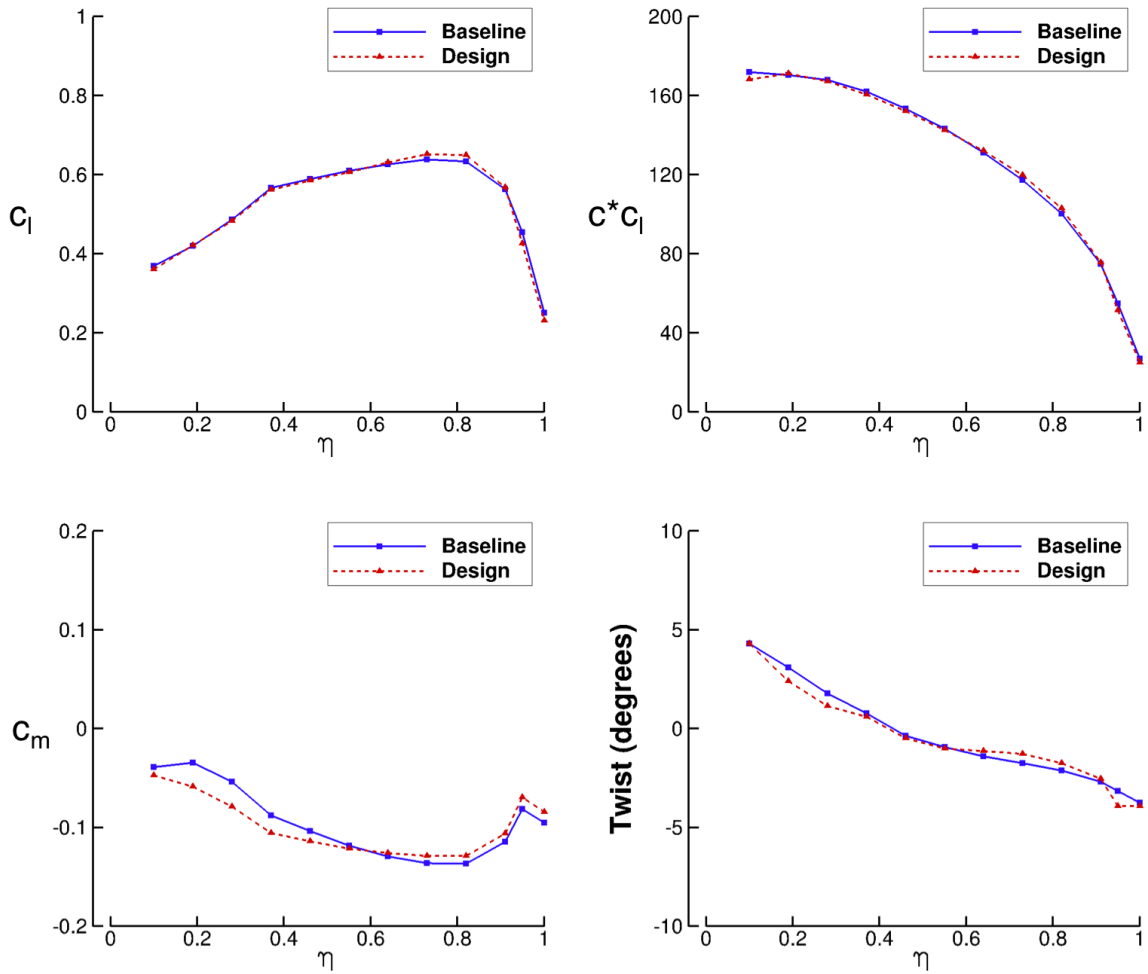
Figure 13. Comparison of spanwise characteristics of the initial CRM (Baseline) and CODISC optimized (Design) configurations at Station 3 (top) and Station 9 (bottom).
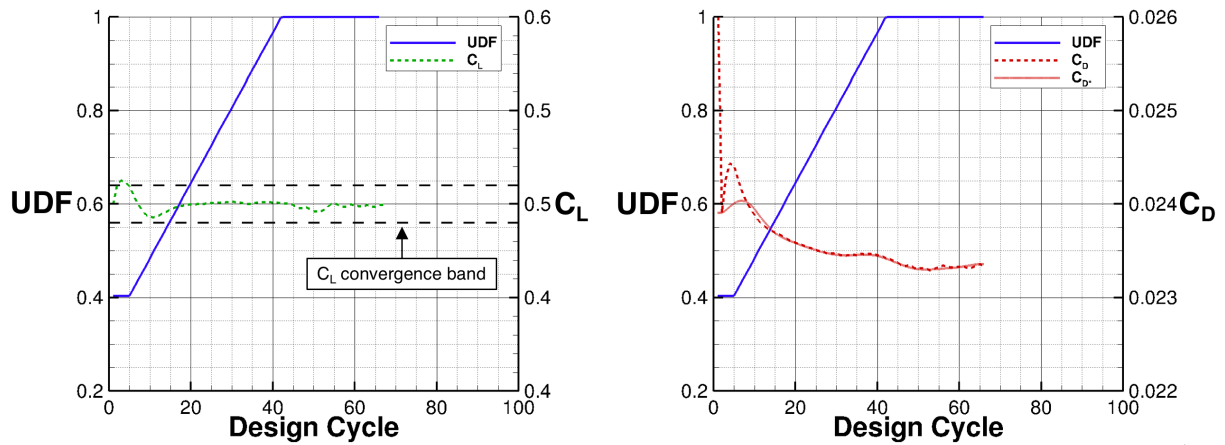
Figure 14. History of the optimized variable (UDF) and the total forces (lift on left, drag on right) during the CODISC optimization process.

Figure 15. Spanwise distribution of the UDF variable.

Figure 16. Drag polar showing near-cruise off-design performance of the two optimized designs compared to the baseline CRM.
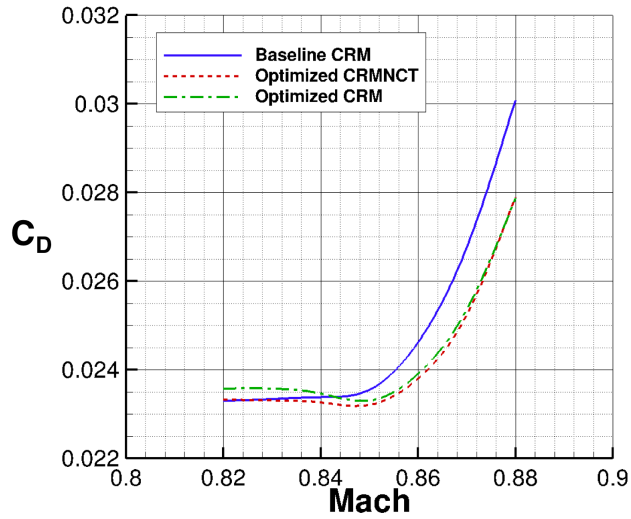
Figure 17. Drag rise plot comparing the two optimized designs to the baseline CRM.
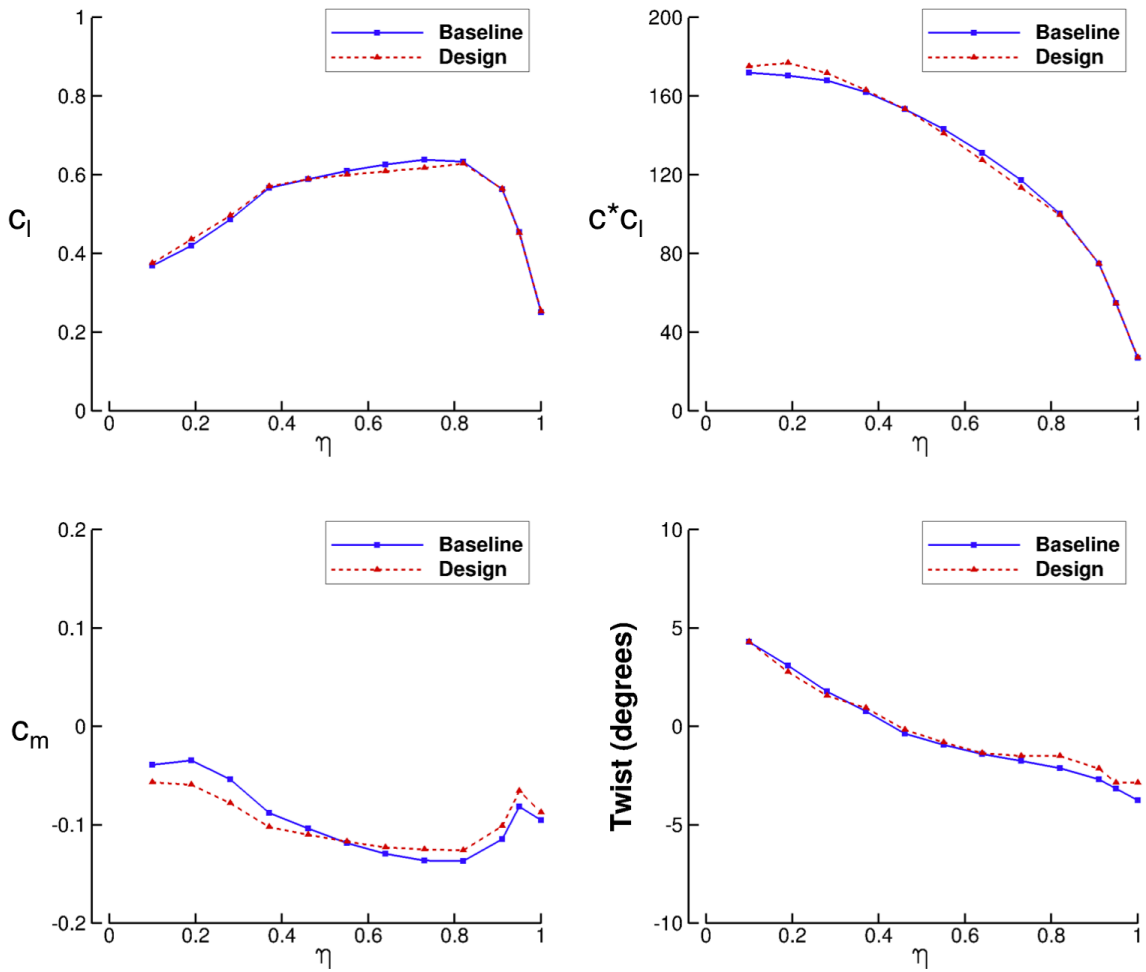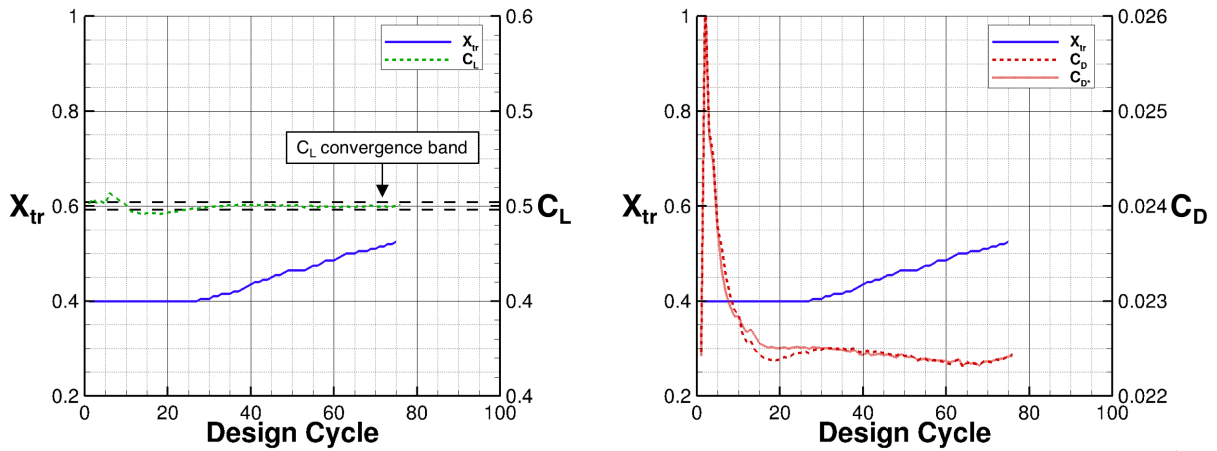

Figure 18. Comparison of the pressure distribution (left) and airfoil shape (right) of the initial CRM (Baseline) and laminar CODISC optimized (Design) configurations at Station 3 (top) and Station 9 (bottom).

Figure 19. Comparison of spanwise characteristics of the initial CRM (Baseline) and CODISC optimized (Design) configurations at Station 3 (top) and Station 9 (bottom).

Figure 20. History of the optimized variable (X_{tr}) and the total forces (lift on left, drag on right) during the CODISC optimization process for laminar design.
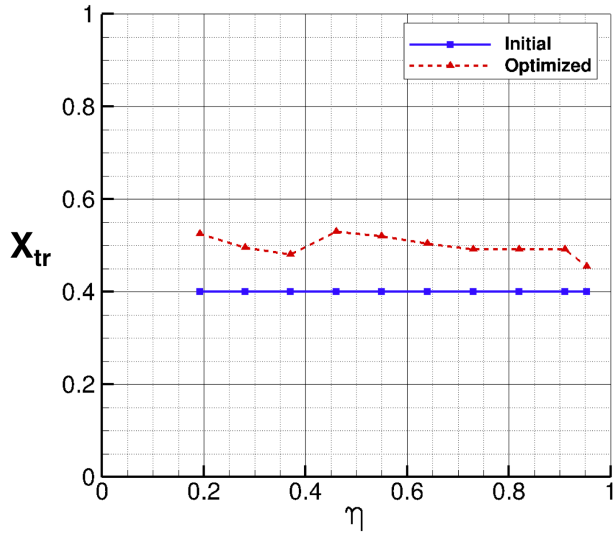
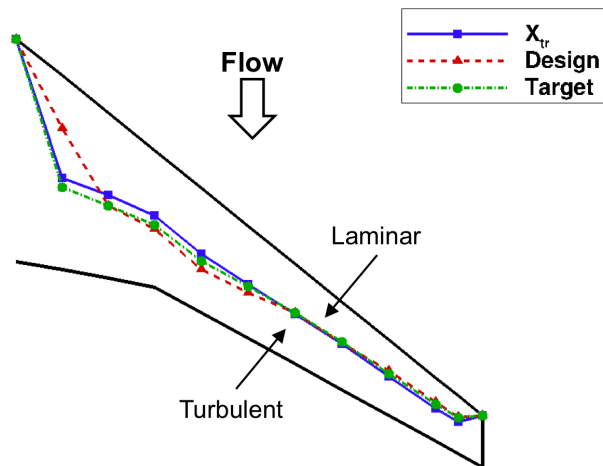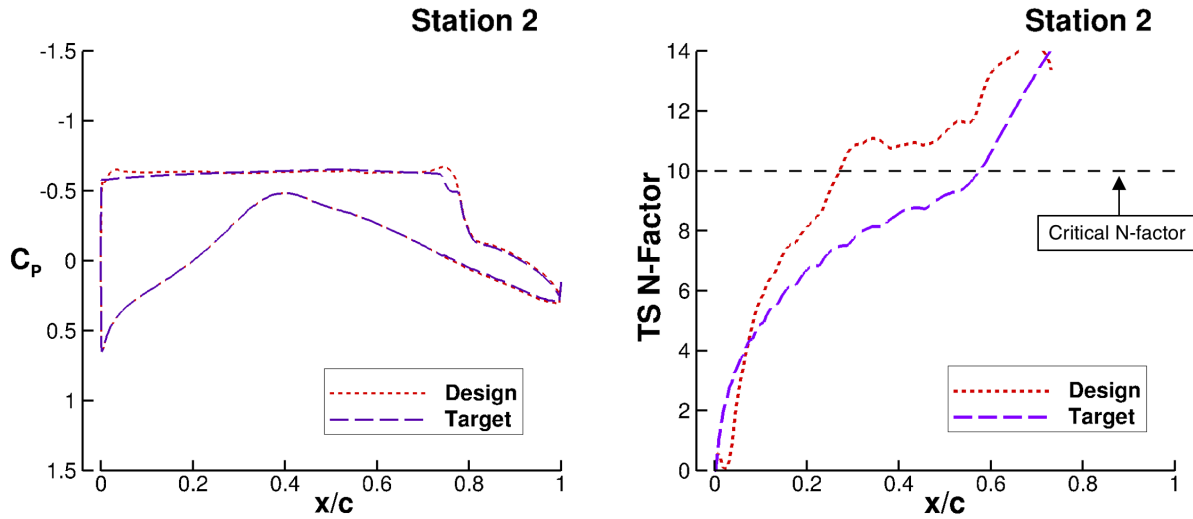**Figure 21.** Spanwise distribution of the X_{tr} locations.

Figure 22. Planform view showing the transition front on the laminar CODISC design. Compares transition front of the Xtr locations (blue, X_{tr}) and fronts calculated with LASTRAC from the final design flow solution (red, Design) and the target pressure distribution (green, Target).

Figure 23. Comparison of the pressure distribution (left) and the resulting TS N-factor growth (right) for the final design flow solution and target pressure distribution at inboard Station 2.

Table 1. Performance comparison of the two optimized turbulent designs and the baseline CRM at the design point.

Configuration	Angle of Attack	C_L	C_D	Drag Reduction
Baseline CRM	1.96 deg.	0.5000	0.02357	
Optimized from CRMNCT	1.96 deg.	0.4999	0.02321	3.6 counts (1.5%)
Optimized from CRM	1.96 deg.	0.5001	0.02330	2.7 counts (1.1%)

Table 2. Performance comparison of the two optimized turbulent designs and the baseline CRM at the limits of the near-cruise off-design conditions.

Condition	Configuration	C_L	C_D	Drag Reduction
+10% Design C_L	Baseline CRM	0.5500	0.02625	
	Optimized from CRMNCT	0.5500	0.02562	6.3 counts (2.4%)
	Optimized from CRM	0.5500	0.02573	5.2 counts (2.0%)
Design C_L	Baseline CRM	0.5000	0.02357	
	Optimized from CRMNCT	0.4999	0.02321	3.6 counts (1.5%)
	Optimized from CRM	0.5001	0.02330	2.7 counts (1.1%)
-10% Design C_L	Baseline CRM	0.4500	0.02161	
	Optimized from CRMNCT	0.4500	0.02159	-0.5 counts (-0.1%)
	Optimized from CRM	0.4500	0.02176	-1.5 counts (-0.7%)